Published in final edited form as:
J Immunol. 2009 April 15; 182(8): 5052–5062. doi:10.4049/jimmunol.0802968.

P2X7 receptor-stimulated secretion of MHC-II-containing exosomes requires the ASC/NLRP3 inflammasome but is independent of caspase-1[1]

Yan Qu[#], **Lakshmi Ramachandra**[**], **Susanne Mohr**[*,+], **Luigi Franchi**[***], **Clifford V. Harding**[**], **Gabriel Nunez**[***], and **George R. Dubyak**[*,#,**,2]

[*] Department of Physiology and Biophysics, Case Western Reserve University School of Medicine, Cleveland OH

[#] Department of Pharmacology, Case Western Reserve University School of Medicine, Cleveland OH

[**] Department of Pathology, Case Western Reserve University School of Medicine, Cleveland OH

[+] Department of Medicine, Case Western Reserve University School of Medicine, Cleveland OH

[***] Department of Pathology, University of Michigan, Ann Arbor, MI

Abstract

We recently reported that P2X7 receptor (P2X7R)-induced activation of caspase-1 inflammasomes is accompanied by release of MHC-II protein into extracellular compartments during brief stimulation of murine macrophages with ATP. Here we demonstrate that MHC-II containing membranes released from macrophages or dendritic cells (DC) in response to P2X7R stimulation comprise two pools of vesicles with distinct biogenesis: one pool comprises 100–600 nm microvesicles derived from direct budding of the plasma membrane while the second pool is composed of 50–80 nm exosomes released from multivesicular bodies (MVB). ATP-stimulated release of MHC-II in these membrane fractions is observed within 15 min and results in the export of ~15% of the total MHC-II pool within 90 min. ATP did not stimulate MHC-II release in macrophages from P2X7R-knockout mice. The inflammasome regulatory proteins, ASC and NLRP3, which are essential for caspase-1 activation, were also required for the P2X7R-regulated release of the exosome but not the microvesicle MHC-II pool. Treatment of BMDM with YVAD-cmk, a peptide inhibitor of caspase-1, also abrogated P2X7R-dependent MHC-II secretion. Surprisingly however, MHC-II release in response to ATP was intact in caspase-1−/− macrophages. The inhibitory actions of YVAD-cmk were mimicked by the pan-caspase inhibitor zVAD-fmk and the serine protease inhibitor TPCK, but not the caspase-3 inhibitor, DEVD-cho. These data suggest that the ASC/NLRP3 inflammasome complexes assembled in response to P2X7R activation involve protease effector(s) in addition to caspase-1 and that these proteases may play important roles in

[1]This work was supported by NIH grants GM36387 to G.R.D., AI035726/AI069085 to C.V.H., AI063331/AI064748 to G.N.

2Address correspondence and reprint requests to: George R. Dubyak, Ph.D., Department of Physiology and Biophysics, Case Western Reserve University School of Medicine, 10900 Euclid Avenue, Cleveland OH, 44120, george.dubyak@case.edu, Phone (216)368-5523, FAX (216)368-3952.

regulating the membrane trafficking pathways that control biogenesis and release of MHCII-containing exosomes.

Introduction

Stimulation of P2X7 purinergic receptors (P2X7R) triggers the rapid assembly of inflammasome signaling complexes (1), that include ASC (2) and NLRP3 (formerly Nalp3 or cyropyrin) (3); these complexes act as signaling platforms to drive the proteolytic activation of caspase-1 and maturation of IL-1β. In a previous study of the mechanisms underlying non-classical IL-β secretion stimulated by activation of P2X7R in murine macrophages, we observed that ATP-induced caspase-1 activation and IL-1β release was temporally correlated with a rapid and robust secretion of MHC-II protein (4). That the ATP-triggered MHC-II export was greatly increased by LPS priming and attenuated by the YVAD caspase-1 inhibitor, suggested the intriguing possibility that caspase-1 inflammasomes play additional roles in the biogenesis and trafficking of MHC-II-enriched membrane compartments. Although rapid perturbation of ion homeostasis is the best-characterized cellular response to P2X7R activation, this ATP-gated nonselective cation channel has also been associated with a diverse array of membrane trafficking responses in immune and inflammatory effector cells (5–8). Major histocompatability complex class II (MHC-II) proteins, which are selectively expressed in professional antigen-presenting cells (APCs) including macrophages, dendritic cells (DCs) and B cells, play critical roles in mediating the presentation of extracellular pathogen-derived and other exogenous proteins to $CD4^+$ T-helper cells. Notably, a previous study by Di Virgilio and colleagues reported that activation of P2X7R potentiated antigen presentation by murine dendritic cells (DC) (9). However, the mechanisms by which P2X7R signaling regulate MHC-II trafficking and antigen presentation remain unclear.

Altered expression of MHC-II-peptide complexes has been associated with various inflammatory and antoimmune diseases (10,11). Unlike the class I MHC molecules which bind antigenic peptides transported into the endoplasmic reticulum (ER), the formation of foreign antigen-class II complexes occurs in the MHC class II containing compartments (MIICs). These MIICs are specialized late endosomes/lysosomes that are enriched in MHC-II protein. Other molecules that are contained within the MIICs include human leukocyte antigen (HLA)-DM, HLA-DO, IFN-γ-inducible lysosomal thiol reductase, and cathepsins which are important for exogenous peptide processing, loading, and editing (12,13). The biogenesis and the plasma membrane expression of peptide-MHC-II (pMHC-II) complexes involve several membrane trafficking pathways including: 1) endocytosis of extracellular foreign protein via the recycling endosomes; 2) formation of lysosome-like MIICs through the fusion of late endosomes that contain exogenous antigens with the *de novo* synthesized MHC-II molecules derived from the Golgi apparatus; and 3) formation of multivesicular bodies (MVBs) generated by inward budding from the limiting membrane of the MIIC organelles and accumulation of these inward buds as intraluminal vesicles (ILV). The pMHC-II complexes are formed via antigen-loading onto the MHC-II pools of both ILVs and the limit membrane of these specialized MVBs. This facilitates delivery of pMHC-II complexes to the cell surface upon exocytotic fusion of the MVBs with the plasma membrane (13–15). Additionally, this exocytosis can result in the direct secretion of the MHC-II containing ILVs into extracellular compartment as so-called exosomes.

Most APCs directly present their antigens to T cells via the cell surface pool of MHC-II. However, increasing evidence indicates that MVB-derived exosomes containing pMHC-II complexes are also competent to promote T-cell activation/proliferation and thereby initiate antigen-specific immune responses *in vivo* (16,17). Various studies have indicated that released exosomes can activate remote T lymphocytes either by direct antigen presentation from the

pMHC-II displayed on the exosomal surface or by a predominant indirect pathway wherein these exosomes are taken up by remote naive DCs for DC-mediated antigen presentation (17–19). Recent studies on exosome biology have expanded their physiological functions to even broader types of intercellular communication, including the exchange of genetic material such as intact mRNAs and microRNAs, transfer of oncogenic growth factor receptors from tumor cells to remote non-transformed cells, trans-infection of T cells by HIV-1 virions packaged within DC-derived exosomes, and transfer of pathogen-associated molecular patterns (PAMPs) between macrophages (20–23).

Intracellular signaling cascades that may regulate the various steps of exosome biogenesis are poorly defined. The formation and secretion of MHC-II-containing exosomes in APCs has been largely viewed as a constitutive pathway. However, recent studies performed in DCs and B cells suggest that both cell surface MHC-II levels and the antigen presentation capacities of released MHC-II containing exosomes are dynamically regulated by various signaling pathways active during particular phases of APC maturation or stimulation (24–26). In contrast to the slow constitutive secretion of exosomes that typically occurs over ~24 – 48 h of media conditioning by cultured APC, recent studies have demonstrated that exosome release can be accelerated by conditions or pharmacological agents that target various signaling pathways (20,27,28).

In this study we extend the analysis of P2X7R-induced release of MHC-II containing membranes in murine primary macrophages and dendritic cells by defining: 1) the basic biophysical and biochemical properties of the released MHC-II vesicles; and 2) the role of particular inflammasome-associated proteins, including ASC, NLRP3, and caspase-1 in the biogenesis/export of these vesicles. In contrast to the slow constitutive MHC-II secretion previously described in DCs and B cells, the ATP-triggered MHC-II release occurred in a very rapid and efficient manner (within 15 min after ATP stimulation) and included both larger (100–600 nm) plasma membrane-derived microvesicles and smaller (50–80 nm) exosome-like vesicles. Moreover, our data indicate that the signaling cascades required for the secretion of MHC-II membranes overlap with, but are distinct from, those required for caspase-1 activation and IL-1β export. Although maximal P2X7R-dependent MHC-II release requires 1) LPS priming, 2) the inflammasome adapter proteins ASC and NLRP3, and 3) effector proteins sensitive to the widely used YVAD-cmk inhibitor of caspase-1, it is not affected by the absence of caspase-1 expression per se. The discrepant effects on ATP-triggered MHC-II release observed with $ASC^{-/-}$ or $NLRP3^{-/-}$ BMDM versus $caspase\text{-}1^{-/-}$ BMDM reveals an additional role for P2X7R-regulated inflammasome adapter proteins other than acting as the molecular platform for caspase-1 maturation.

Materials and Methods

Reagents

Key reagents and their sources were: *Escherichia coli* LPS serotype O1101:B4 (List Biological Laboratories; ATP (Sigma), YVAD-cmk (BACHEM), DEVD-CHO (BioMol), ZVAD-fmk (BioMol), and Na-Tosyl-Phe-chloromethylketone (TPCK) (Sigma). The Cytotoxicity Detection Kit was from Roche. Recombinant murine interferon-γ (IFN-γ) was from Boehringer Mannheim Biochemica. Anti-caspase-1 p10 rabbit polyclonal, anti-cathepsin B goat polyclonal, anti-actin goat polyclonal, anti-LAMP-1 rat monoclonal, and all HRP-conjugated secondary antibodies were from Santa Cruz Biotechnology. The monoclonal 3ZD anti-IL-1β Ab, which recognizes both 33 kDa pro-IL-1β and 17 kDa mature IL-1β in western blot analysis, was provided by the Biological Resources Branch, National Cancer Institute, Frederick Cancer Research and Development Center, Frederick, MD. The mouse mAb KL295 against MHC-IIβ chain ($I\text{-}A^b$ and $I\text{-}A^d$ haplotypes and the rat anti-mouse ASC monoclonal antibody have been previously described (29).

Mouse models and methods for isolation and cell culture of bone marrow-derived macrophages or dendritic cells

C57BL/6 mice were purchased from Taconic, Inc.; P2X7R$^{-/-}$ mice were originally provided by Pfizer Global Research and Development, Pfizer Inc. and then backcrossed into a pure C57BL/6 background for >12 generations from a P2X7R$^{-/-}$ mouse strain described previously (30). ASC $^{-/-}$ and NLRP3$^{-/-}$ mice (C57BL/6 background) were generated as described previously in the Nunez laboratory at University of Michigan. Caspase-1$^{-/-}$ mice (C57BL/6 background) that were backcrossed for five generations with the C57BL/6J strain were obtained from Richard Flavell (Yale University). All experiments and procedures involving mice were approved by the Institutional Animal Use and Care Committees of either Case Western Reserve University or University of Michigan.

Bone marrow-derived macrophages (BMDM) were isolated by previously described protocols (31). Mice were euthanized by CO_2 inhalation. Femurs and tibia were removed, briefly sterilized in 70% ethanol, and PBS was used to wash out the marrow cavity plugs. The bone marrow cells were resuspended in DMEM (Sigma-Aldrich) supplemented with 25% L cell-conditioned medium, 15% calf serum (HyClone Laboratories), 100 U/ml penicillin, and 100 μg/ml streptomycin (Invitrogen Life Technologies), plated onto 150 mm dishes, cultured in the presence of 10% CO_2. After 5–9 days, the resulting BMDM were detached with PBS containing 5 mM EDTA and 4 mg/ml lidocaine (31), replated into six-well or 12-well plates, and used within 10 days. A similar method was used to generate dendritic cells (DCs): the bone marrow cells were cultured in DMEM supplemented with 3% ~5% J558L cell-conditioned medium which contains GM-CSF, 15% calf serum, 100 U/ml penicillin, and 100 μg/ml streptomycin. Culture medium was changed after 3 days post isolation, and the cells were ready to be used after 7 days post isolation.

Western blot analyses for caspase-1 activation and release, IL-1β processing and secretion, exocytosis of secretory lysosomes, and plasma membrane microvesicle shedding

BMDM were routinely seeded in 6-well plates to a cell density of ~2×10^6/well and stimulated with 2 ng/ml IFN-γ for 16–18 hr prior to LPS priming and ATP stimulation. IFN-γ treatment is required to up-regulate expression of MHC-II in BMDM. After IFN-γ priming, the culture medium was replaced with fresh medium supplemented with or without 1 μg/ml LPS. In some experiments, cells were pretreated with various pharmacological inhibitors prior to, and during, LPS priming. Cell were primed with LPS for 4 hr at 37 °C, followed by washing once with PBS and transfer to 1 ml of basal saline solution (BSS) assay medium containing 130 mM sodium gluconate, 5 mM KCl, 20 mM NaHEPES, 1.5 mM $CaCl_2$, 1.0 mM $MgCl_2$, pH 7.5 supplemented with 5 mM glucose, 5 mM glycine, and 0.01% BSA. Experiments testing effects of extracellular Ca^{2+} on MHC-II release utilized BSS with no added $CaCl_2$. Cells were then equilibrated for an additional 5 min at 37 °C prior to stimulation with ATP. To terminate the release reaction, the entire 1 ml of extracellular medium was transferred to a tube on ice, while the cell monolayer was rapidly washed once with 1 ml ice-cold PBS, and then lysed by addition of 150 μl RIPA extraction buffer (1% NP-40, 0.5% Na-deoxycholate, 0.1% SDS, pH7.4 in PBS) containing PMSF, leupeptin, and aprotinin. For processing of extracellular media, the collected 1 ml samples were centrifuged at the 10,000 ×g for 10 sec to remove any detached cells followed by transfer of the supernatant to a fresh tube. The supernatant was concentrated by TCA precipitation using 72 μl of 100% TCA and 15 μl of 10% cholic acid per 1 ml of extracellular media. The precipitated pellets were washed 3 times with 1 ml acetone, dissolved in 10 μl 0.2 M NaOH, diluted with 35 μl H_2O, supplemented with 15 μl of 4×SDS-PAGE sample buffer, and boiled for 5 min. For processing of cell lysates, the 150 μl RIPA extracts were combined with any detached cells from the extracellular media, re-centrifuged, and supernatants transferred to fresh tubes. 45 μl of cell lysate was supplemented with 15 μl of 4×SDS-PAGE sample buffer and boiled for 5 min. Extracellular media and cell lysates were

processed by SDS-PAGE, electrophoretic transfer PVDF membranes, and standard western blot protocols as described previously (32). Primary antibodies were used at the following concentrations: 5 μg/ml for IL-1β, 1 μg/ml for caspase-1, 1 μg/ml for actin, 0.04 μg/ml for LAMP-1, 1 μg/ml for cathepsin B, and 0.8 μg/ml for MHC-II. HRP-conjugated secondary antibodies were used at a final concentration of 0.13 μg/ml.

Purification of microvesicles and exosomes

All experiments that characterized the MHC-II containing membrane vesicles by centrifugation analysis utilized BMDM or BMDC grown in 150 mm dishes to a cell density of ~ 10×10^7. The BMDM were stimulated with 2 ng/ml IFN-γ for 16–18 hr prior to LPS priming and ATP stimulation. Culture medium was replaced with fresh medium supplemented with or without 1 μg/ml LPS. The cells were primed with LPS for 4 h at 37 °C, followed by washing once with PBS and transfer to 10 ml BSS assay medium. Cells were then equilibrated for an additional 5 min at 37 °C prior to stimulation with 5 mM ATP for indicated times. The collected medium was immediately transferred into a tube containing PMSF, leupeptin, and aprotinin on ice, and then followed by sequential centrifugation at 4 °C for 10 min at 300×g, 20 min at 1200×g, 30 min at 10,000×g (Sorvall SS-34 rotor), and 1 h at 100,000×g (Beckman Ti 90 rotor). The pellets from 10,000×g and 100,000×g spins were re-suspended in 1 ml PBS, laid on top of linear sucrose density gradient (see below), and then centrifuged at 100,000×g for 15~16 h (Beckman SW28 rotor). For western blot analysis of the microvesicles and exosomes, the collected medium was sequentially centrifuged at 4 °C for 10 min at 300×g, 20 min at 1200×g, 30 min at 10,000×g (Sorvall SS-34 rotor), 15~16 h at 100,000×g (Beckman Ti 90 rotor). The pellets collected from 10,000×g and 100,000×g were re-suspended in 1 ml PBS, precipitated by TCA and analyzed by western blot.

Equilibrium sucrose density gradient centrifugation

Continuous sucrose density gradient were generated by layering 1 ml aliquots of 12 sucrose solutions (65%, 60%, 55%, 50%, 45%, 40%, 35%, 30%, 25%, 20%, 15%, 10% in 20 mM HEPES/NaOH, pH7.2) upon one another successively in a 15 ml ultraclear polyallomer centrifuge tube (Beckman), with the heaviest layer at the bottom and the lightest layer at the top. The tube was incubated at 4 °C for 5–6 h to allow diffusional mixing to establish a continuous sucrose density gradient. To perform sucrose density gradient centrifugation, the collected extracellular medium from BMDM or BMDC cultures was sequentially centrifuged for 10 min at 300×g and 20 min at 2000×g to eliminate detached intact cells and large debris. The resulting supernatant was concentrated for ~1.5–2 h at 3000×g using CENTRIPREP (Ultracel YM-3 membrane, Millipore), which decreased the media volume from 10 ml to ~1 ml. The concentrated extracellular supernatant was then loaded on top of the pre-equilibrated sucrose density gradient, and centrifuged at 100,000×g for 15 h (Beckman SW28 rotor). 1 ml fractions were taken from the top of the tube and the density of each collected fraction was measured by direct weighing of the 1 ml aliquot. After weighing, each fraction was diluted with 1 ml PBS and then precipitated with TCA. The precipitated proteins were analyzed by western blot for various proteins (MHC-II, caspase-1, IL-1β, LAMP1, actin) as indicated in particular figures.

Electron Microscopy

Purified microvesicles and exosomes were fixed in a mixture of 2.0% glutaraldehyde and 4% sucrose in a 0.05 M phosphate buffer, pH 7.4, for 2 h and then postfixed in 1% osmium tetroxide for 1 h at room temperature. Samples were then block-stained in 0.5% aqueous uranyl acetate, dehydrated in ascending concentration of ethanol and embedded in Epon 812. Ultrathin sections (60 nm thicknesses) were cut on a RMC MT6000-XL microtome and stained with 2%

uranyl acetate in 50% methanol and with lead citrate, and then examined in a JEOL 1200EX electron microscope at 80 kV.

Measurement of LDH Release

Basal and ATP-stimulated LDH release was measured as described previously using the Cytotoxicity Detection Kit from Roche (33). The results are expressed as a percentage of total LDH released, which was obtained by dividing the amount of LDH detected extracellularly by the sum total of LDH detected within the cell and the amount detected in extracellular medium, and multiplying by 100.

Results

P2X7R activation stimulates the rapid release of MHC-II membranes from inflammatory murine macrophages

We previously reported that activation of P2X7R can induce efficient intracellular inflammasome assembly and maturation of IL-1β, followed by rapid secretion of the mature IL-1β and activated caspase-1 to the extracellular compartment (4). Concurrent with these responses, we also observed an ATP-induced rapid release of MHC-II. We compared ATP-induced MHC-II secretion in bone marrow-derived macrophages (BMDM) bathed in NaGluconate BSS (as an optimal experimental test solution for P2X7R activation (33) versus standard DMEM (as a NaCl-based physiological tissue culture medium). As indicated in Fig. 1A, under both test conditions a rapid secretion of MHC-II was initiated during the first 15 min of exposure to ATP, and this was followed by a sustained accumulation over the next 75 min. Consistent with our previous observations that extracellular Cl^- decreases the efficacy of P2X7R as an activator of caspase-1 inflammasomes (33), we observed attenuated, but still significant, MHC-II release and delayed caspase-1 activation when BMDM were stimulated with ATP in DMEM versus NaGluconate BSS. We used semi-quantitative western blot analysis (Figs. 1B and 1C) to compare the amounts of secreted MHC-II as a percentage of the total intracellular MHC-II in BMDM pre-treated with the different priming stimuli. In cells primed with LPS, activation of P2X7R stimulated the release of 1.3±0.1% (n=8) the total MHC-II pool within 15 min after ATP incubation. By 30 min post ATP stimulation, the accumulation of secreted MHC-II reached 5.3±0.5% (n=8) of the total cell content. By 90 min after addition of ATP, 15.3±0.1% (n=8) of the total cellular MHC-II pool was transferred to the extracellular compartment (Fig. 1D).

In the absence of acute ATP stimulation, the IFN-γ- and LPS-primed BMDM did not release measurable MHC-II during 90 min test incubations (Fig. 1E). We also observed no MHC-II release in BMDM derived from P2X7R-null mice that were primed with IFN-γ and LPS and stimulated with 5 mM ATP for up to 90 min (Fig. 1F). This is notable because murine macrophages express multiple P2 receptors, in addition to P2X7R, that are also activated by extracellular ATP and other nucleotides (34). Similar levels of total MHC-II were expressed in the P2X7-knockout BMDM. As previously described (4,35,36), the P2X7R-deficient macrophages exhibited no caspase-1 activation response to extracellular ATP.

Consistent with previous findings by us (33) and others (37) sustained activation of P2X7R for 90 min induced significant macrophage death but only after priming with LPS. ATP-induced cell death, as indicated by LDH release, was 38% in IFN-γ plus LPS-primed cells versus 5% in cells primed with IFN-γ only (Supplementary Data, Fig 1). At the 30 min post ATP, the LDH release was proportionately lower (11% in IFN-γ/LPS-primed versus 5% in IFN-γ-primed l cells). ATP-induced cell death was strictly dependent on expression of P2X7R as indicated by the minor LDH release (4% at 90 min) in IFN-γ/LPS-primed BMDM from P2X7R-knockout mice.

Distinct regulatory roles of the inflammasome proteins ASC, NLRP3, and caspase-1 in P2X7R-stimulated MHC-II release

We examined MHC-II release in non-LPS-primed versus LPS-primed macrophages in response to P2X7R stimulation over a 90 min test period. When compared to LPS-primed cells, both the kinetics and extent of ATP-induced MHC-II release were markedly attenuated in the non-LPS primed macrophages. At 30 min post ATP, the non-primed BMDM released 1±0.3% (n=8) of their MHC-II in contrast to the 5.3+0.5% (n=8) secreted by the LPS-primed cells. Even after 90 min of ATP stimulation, only 3.8+1.8% (n=8) of the MHC-II pool was externalized by the non-primed cells relative to the 15.3±0.1% (n=8) release observed in the primed BMDM (Figs. 2A and 2B). This suggests that LPS-dependent signaling cascades which are required for efficient coupling of P2X7R to caspase-1 inflammasome assembly also facilitate ATP-stimulated MHC-II secretion.

Inclusion of YVAD-cmk, an inhibitor of active caspase-1, during ATP stimulation of the LPS-primed BMDM significantly altered the kinetics and magnitude of MHC-II secretion (Figs. 2A and 2B). Only 0.3±0.2 % (n=6) of the MHC-II pool was secreted during 30 min of ATP stimulation in the presence of YVAD-cmk versus 5.3+0.5% (n=8) release in its absence. Prolongation of the ATP stimulation duration to 90 min did not overcome this blocking effect; at this time point, YVAD-treated cells released 1±0.5% (n=6) of their MHC-II relative to the 15.3±0.1% (n=8) release in its absence. These findings suggested a potential role of active caspase-1 in regulating the MHC-II trafficking response to P2X7R stimulation. To investigate whether caspase-1 is indeed essential for the P2X7R-stimulated MHC-II release, we compared the kinetics and magnitudes of ATP-induced MHC-II release in BMDM derived from wildtype versus caspase-1-null mice. Surprisingly, the absence of caspase-1 only modestly affected the kinetics and extent of ATP-triggered MHC-II secretion (Fig. 2C and 2D). A reduction in MHC-II release from the knockout cells was observed at 30 min (2.6+0.3%, n=5 versus 5.3+0.5% (n=8) in the control macrophages). However, with more prolonged ATP stimulation periods (90 min), the caspase-$1^{-/-}$ and wildtype BMDM released comparable amounts of MHC-II (15.5 +1.5%, n=5 versus 15.3±0.1%, n=8 in knockout versus control, respectively). Notably, treatment of the caspase-1 knockout macrophages with YVAD-cmk markedly inhibited ATP-stimulated MHC-II secretion at all time points (Figs. 2C and 2D); released MHC-II at 90 min was 5±1% (n=4) in the presence of the peptide versus 15.5+1.5% (n=5) in its absence.

Peptide inhibitors of the various caspases are not completely selective (38,39). To test the selectivity of YVAD-cmk as an inhibitor of ATP-stimulated MHC-II release in wildtype BMDM, we also examined the effects of zVAD-fmk, a pan-caspase inhibitor, TPCK, a serine protease inhibitor, or DEVD-cho, a caspase-3 inhibitor (Fig. 2E). The zVAD-fmk and TPCK, but not DEVD-cho, markedly attenuated MHC-II release (measured at 30 min) and completely abrogated caspase-1 activation in response to P2X7R activation. The effects of these protease inhibitors on MHC-II release were not due to non-specific toxic effects or suppression of proximal P2X7R activation because none of the agents blocked ATP-stimulated exocytosis of secretory lysosomes (as assayed by cathepsin B release) (Fig. 2E). We have previously reported that P2X7 receptors trigger the mobilization of secretory lysosomes from macrophages via Ca^{2+}-dependent signaling that can be dissociated from the parallel pathway which couples these receptors to inflammasome activation (4).

To further dissect the possible role of inflammasome complex assembly upstream of caspase-1 in regulating P2X7R-dependent MHC-II secretion, we used BMDM derived from wildtype (WT), ASC-null, and NLRP3-null mice for comparative analyses of MHC-II release kinetics during ATP stimulation periods ranging from 15–60 min (Figs. 3A and 3B; the WT and caspase-1-null quantitative data sets from Fig 2D have been re-plotted for comparison). At all time points, P2X7R-dependent MHC-II release was markedly decreased in $ASC^{-/-}$ and $NLRP3^{-/-}$macrophages compared with WT cells or caspase-$1^{-/-}$ cells. At 60 min, the

extracellular content of MHC-II as a percentage of the total cellular MHC-II pool was 0.1±0.1% (n=7) for ASC$^{-/-}$ cells and 1.2±0.2 (n=7) for NLRP3$^{-/-}$ macrophages which contrasted with 7.8+1.6% (n=8) for wildtype cells. Notably, the release of MHC-II from ASC-null cells measured at 30 min was greater (1±0.5%, n=7) than at 60 min; this suggests that previously released MHC-II might be re-accumulated or metabolically cleared in the absence of sustained export of MHC-II. As noted previously, the ATP-stimulated caspase-1$^{-/-}$ cells released MHC-II at levels were only modestly different from those in WT cells (no difference at 15 min, 45% decrease at 30 min, 75% increase at 60 min). We verified that the BMDM derived from these four different mouse strains expressed similar amounts of total MHC-II protein (Fig. 3C). Moreover, BMDM derived from the ASC- or NLRP3- deficient mice were not compromised in P2X7R-stimulated secretory lysosome exocytosis, which is strictly dependent on the influx of extracellular Ca^{2+} triggered by P2X7R (4), but were completely deficient in P2X7R-induced inflammasome activation and release of active caspase-1 (Fig. 3D)..

MHC-II released in response to P2X7R activation is contained in microvesicles and exosome-like vesicles with distinct morphologies

Previous studies have demonstrated that MHC-II constitutively released from dendritic cells or B cells is predominantly associated with membranous exosome vesicles derived from the intraluminal vesicles of MIIC or other MVB-like organelles (40,41). To further characterize the nature of the MHC-II pool(s) secreted in response to P2X7R activation, we tested whether the released MHC-II is associated with membrane compartments that exhibit the established biophysical properties of exosomes by using equilibrium sucrose density gradient centrifugation. As indicated in Fig. 4A, all MHC-II released in response to ATP was localized to sucrose densities ranging between 1.08 and 1.15 g/ml, consistent with the buoyant density of exosomes reported in previous studies (16,20,41). In contrast, the lysosomal protease cathepsin B, a soluble protein released via secretory lysosome exocytosis stimulated by P2X7R, was exclusively localized at the top of the sucrose gradient. Interestingly, we also observed that subfractions of LAMP-1, caspase-1 p10 subunit, and mature IL-1β colocalized with MHC-II in the >1.1 g/ml density bands of the sucrose gradient. This further supports our previous hypothesis that MVB-derived exosomes may comprise a non-classical secretory pathway for release of mature IL-1β and active caspase-1 from murine macrophages.

Activation of P2X7R is also known to trigger rapid blebbing of the plasma membrane (5) and shedding of such blebs as released microvesicles or microparticles (6–8,42). To test the contribution of shed microvesicles versus exosomes to the MHC-II fractions observed in sucrose gradients, we collected the extracellular media from BMDM stimulated by ATP (precleared of detached cells and large debris by successive centrifugation at 300×g and 1200×g) and then isolated an initial pellet fraction that sedimented at 10,000×g and a secondary pellet that sedimented at 100,000×g. Electron microscopic analysis of these two sedimentable membrane fractions (Fig. 4C) revealed that the 100,000×g pellet contained homogeneously sized and optically dense vesicles ranging from 50–80 nm in diameter, which is consistent with the reported morphological properties of exosomes. In contrast, the 10,000×g pellet contained a more heterogeneous component of membrane vesicles that ranged in size between 100–600 nm in diameter.

Each resuspended membrane fraction was also loaded on linear sucrose density and re-centrifuged at 100,000×g for 16 hr. As shown in Fig. 4B, MHC-II similarly accumulated in the 1.11 – 1.14 g/ml density fractions in gradients containing either 10,000×g pellets which represent the presumed microvesicle pool, or the 100,000×g pellets which represent the putative exosome pool. Thus, the MHC-II released in response to P2X7R activation appears to be associated with two different membrane compartments that have distinct biogenesis: microvesicles and exosomes. Moreover, although the two membrane compartments have

different masses, they have similar densities. Hereafter, we refer to the 10,000×g pellet fraction as MHC-II microvesicles and the 100,000×g pellet fraction as MHC-II exosomes. We further characterized the ATP-induced MHC-II microvesicle and exosomes for the presence of LAMP-1 and actin, two other marker proteins previously described in some but not all types of released exosomes (40,41). Both proteins were observed in MHC-II exosomes and MHC-II microvesicles (Fig. 5A) albeit with markedly lower levels of LAMP-1 in the exosome pool at 15 min, but not 30 min, post ATP stimulation.

ASC and NLRP3 are required for the release of MHC-II exosomes but not MHC-II microvesicles in response to P2X7R stimulation

We compared the distributions of MHC-II microvesicles and MHC-II exosomes released from WT, $ASC^{-/-}$, and $NLRP3^{-/-}$ macrophages subjected to identical ATP stimulation periods of 30 min. Figs. 5B and 5C show that similar amounts of MHC-II microvesicles (also positive for LAMP-1 and actin) were released by ATP-stimulated BMDM derived from WT, $ASC^{-/-}$, or $NLRP3^{-/-}$ mice. Conversely, the P2X7R-dependent release of MHC-II exosomes (also containing LAMP-1 and actin markers) from $ASC^{-/-}$ and $NLRP3^{-/-}$ macrophages was greatly reduced relative to that measured in the wildtype cells. Thus, the ASC and NLRP3 inflammasome proteins play critical roles in coupling P2X7R signaling to the biogenesis/export of MVB-derived exosomes, but not the shedding of plasma membrane microvesicles.

Immature and mature dendritic cells also rapidly release MHC-II membrane vesicles in response to extracellular ATP

DCs have been studied extensively to define the mechanisms that underlie exosome formation/secretion and the intracellular trafficking of MHC-II molecules (26,43). We investigated whether murine bone marrow-derived DCs might also rapidly release membranes that contain MHC-II in response to external stimuli such as ATP. As illustrated in Fig. 6A, ATP-induced caspase-1 inflammasome activation and IL-1β maturation were strictly dependent on LPS priming of DC prior to ATP stimulation. Rapid accumulation of extracellular LAMP-1 was also triggered by ATP in DCs. Both immature DCs (non-LPS primed condition) and mature DCs (24 h LPS primed condition) expressed similar levels of MHC-II; this high constitutive expression of MHC-II distinguishes DCs from macrophages which express significant MHC-II only after stimulation with IFN-γ. In contrast to macrophages (Fig. 1E), both the immature DCs and mature DCs exhibited substantial rates of basal or constitutive secretion of MHC-IIin the absence of ATP stimulation (Fig 6E). However, ATP induced a marked increase in MHC-II release concurrently with caspase-1 activation and IL-1β export.

We tested whether the ATP-stimulated MHC-II membranes rapidly released from mature DC are similar in buoyant density to the exosomes constitutively secreted from both immature and mature DC. In the absence of external stimuli, both the immature DCs (no LPS priming) and mature DCs (24 hr LPS priming) constitutively secreted MHC-II during 24 of medium conditioning and this MHC-II was predominantly distributed in the 1.09–1.14 g/ml regions of sucrose gradients (Fig. 6B). Mature DC also released a modest amount of MHC-II vesicles with similar density characteristics even during short-term (20 min) medium conditioning in the absence of ATP stimulation (Fig. 6C). However, inclusion of ATP during this acute 20 min incubation significantly increased this extracellular MHC-II membrane pool. Finally, parallel samples of extracellular medium from ATP-stimulated mature DC were supplemented with or without Triton X-100 prior to loading on the sucrose gradients. Fig. 6D shows that the distribution of released MHC-II was maximal at the 1.14 g/ml region of the sucrose gradient while the triton-treated MHC-II fraction was largely shifted to the soluble, low density (<1.03 g/ml) region. This further indicated that the MHC-II released from DC in response to brief ATP stimulation is contained within membrane s that have the same buoyant density as exosomes constitutively released from immature or mature DC.

Discussion

This study provides a detailed characterization of P2X7R-stimulated release of MHC-II-containing membranes from murine macrophages and DC in the context of the overall proinflammatory response that involves rapid assembly of the ASC/NLRP3 inflammasomes that control caspase-1 activation. Our data indicate that the rapid MHC-II secretion triggered by P2X7R is associated with two types of membrane compartments: microvesicles and exosomes. Based on biochemical and biophysical analysis, we were able to distinguish between ATP-induced microvesicles and exosomes. While both contain MHC-II and exhibit similar densities each is distinguished by a different morphology, mass, and intracellular biogenesis. Electron microscopic images indicated that the plasma membrane-derived microvesicles are heterogeneous in size (100 nm to 600 nm in diameter) while the MVB-derived exosomes are smaller and much more homogeneous in size (50–80 nm in diameter). Using both pharmacological and genetic approaches, we determined that the inflammasome proteins, ASC and NLRP3, play critical roles in regulating the release of MHC-II exosomes independently of their parallel function as key molecular mediators of the caspase-1 activation response to P2X7R signaling.

Plasma membrane-derived microvesicles versus MVB-derived exosomes as a source of extracellular MHC-II

We (33) and others (37) have reported that sustained P2X7R activation triggers significant death of LPS-primed macrophages in a time frame similar to that characterizing the release of MHC-II. However, the ATP-triggered microvesicles and exosomes are morphologically distinct from apoptotic bodies which are 1–4 μm in diameter (44). Previous analyses of exosomes constitutively secreted by DCs and B cells indicated that several MIIC membrane proteins, including LAMP-1, are found mainly on the limiting membrane of MVBs and are minimally detectable in the secreted exosomes (45). We observed that LAMP1 and actin were associated with the ATP-induced exosomes but that the abundance of these markers increased with the duration of the ATP stimulus. In contrast, both LAMP-1 and actin were present in ATP-induced microvesicles even at the earliest time points of isolation. This indicates that the plasma membrane component of LAMP-1, as well as the underlying actin cytoskeleton, can be incorporated into the plasma membrane blebs that rapidly form in response to P2X7R activation and then scission away from the cell surface as released microvesicles. The enrichment of LAMP-1 and actin within the exosome pool observed with longer ATP stimulation suggests that plasma membrane-associated proteins are trafficked into endosomes during the early phase of P2X7 activation, incorporated into the ILV of MVBs, and then secreted as exosomes following MVB exocytosis. Recent studies have indicated that both MHCII and LAMP-1 associated with secretory lysosomes can be rapidly incorporated into the plasma membrane of human monocytes in response to Ca^{2+} ionophore treatment (46).

Multiple studies have shown that antigen-loaded exosomes can be rapidly taken up by naive DCs and macrophages remote from the origin of exosome generation (17–19). In our experimental cell culture model it is possible that MHC-II membranes released at the earlier times following the ATP stimulus are resequestered by viable macrophages at later times. In particular, MHC-II microvesicles initially mobilized by inflammasome-independent mechanisms may be progressively cleared by cells that lack the ability for sustained production and release of MHC-II exosomes. This may underlie the reduced levels of extracellular MHC-II observed at 60 or 90 min versus earlier times in some experiments with ASC-/NLRP3-null macrophages (Figs. 3A and B) or YVAD-treated cells (Figs. 2A and B).

Intracellular signaling cascades that regulate the formation of microvesicles and exosomes

The molecular mechanisms that underlie MHC-II trafficking within the endocytic pathway and the sorting signals involved in MVB formation have not been completely defined. Previous studies have demonstrated that the LPS-induced maturation of DCs regulates the cell surface level of MHC-II via a ubiquitination-based mechanism which provides critical signals for both efficient endocytosis from the plasma membrane and cargo protein sorting into the luminal vesicles of MVBs (24) (25). In murine macrophages, LPS-dependent signaling is necessary for the P2X7R-coupled inflammasome activation that results in processing and release of IL-1β and IL-18 (4,32). Our new data (Fig. 2) indicate that LPS-dependent signals are essential for the optimal coupling of P2X7R to MHC-II trafficking and export. That the release of LAMP-1 positive MHC-II exosomes, but not MHC-II microvesicles, is abrogated in ASC- and NLRP3-deficient macrophages supports a model wherein ASC and NLRP3 play specific roles in regulating MVB formation and exosome secretion in response to P2X7R activation and perhaps other “danger stimuli” that trigger assembly of ASC/NLRP3 inflammasomes. In contrast, P2X7R-dependent induction and release of plasma membrane microvesicles occurs independently of inflammasome assembly. Fang et al. have recently reported that higher-order oligomerization and plasma membrane binding are sufficient to direct the HIV Gag proteins for budding and exosomal sorting (28). This suggests that protein aggregates which accumulate at the plasma membrane or at the limiting membrane of MVBs may comprise one mechanism for cargo sorting into the intraluminal vesicles of the MVBs. Time-lapse confocal analysis of human THP-1 cells stably expressing ASC-GFP fusion protein has demonstrated the formation of a large supramolecular assembly of ASC oligomers, termed the pyroptosome, in response to various proinflammatory stimuli (47). It is possible that the cytosolic oligomerization of inflammasome complex proteins may additionally provide budding/exosomal sorting signals that accelerate the formation of the MVB-derived exosomes containing MHC-II.

The surprising finding that deficiency of caspase-1 had no major effect on ATP-triggered MHC-II release suggests a regulatory role for ASC/NLRP3 inflammasome complexes in functions other than caspase-1 activation. Human macrophages infected with Shigella flexneri exhibit a necrosis-like cell death response which is dependent on ASC and NLRP3, but is independent of caspase-1 and IL-1β (48). Likewise, autophagy resulting from Shigella infection in macrophages provides protection against pyroptotic death and is observed in the absence of caspase-1 and NLRC4, but not ASC (49). Our observation that ATP-induced MHC-II secretion was insensitive to genetic deletion of caspase-1 but sensitive to zVAD-fmk and TPCK, which are widely used pharmacological inhibitors of proteases, indicates that proteases other than caspase-1 may act either upstream or downstream of ASC/NLRP3 inflammasome assembly. The ability of zVAD-fmk and TPCK to mimic the actions of YVAD-cmk suggests that the reactive fluoro-or chloro-methylketone moieties of these inhibitors (38) may underlie their common ability to suppress these putative proteases. Notably, destabilization of phago-lysosomes, and release of lysosomal proteases into the cytosol, has been recently identified as a major mechanism by which multiple particulate stimuli, including silica crystals, alum, and amyloid-beta aggregates, trigger assembly of ASC/NLRP3 inflammasomes (50,51).

The local composition of lipids, especially cone-shaped lipids such as ceramide or lysophosphatidic acid, can rearrange the spatial organization of membrane bilayer leaflets depending on pH and thereby drive vesicle budding by inducing subdomains with curvature that is different from the adjacent planar membrane leaflet (52). In this regard, Trajkovic et al. (53) have reported that cargo proteins in oligodendrocytes can segregate into distinct subdomains of endosomal membranes and that sorting of these proteins into a subset of MVBs occurred by an invagination mechanism independent of the ESCRT (endosomal sorting complex required for transport) machinery usually associated with MVB biogenesis. Rather, this ESCRT-independent process required lipid raft-based microdomains enriched in the

sphingolipid ceramide. It is possible that P2X7R-activated lipases may mediate similar alterations in local lipid composition which initiate or accelerate the formation of microvesicles at the plasma membranes or ILVs/exosomes at endosomal membranes.

Potential physiological functions of MHC-II exosomes and MHC-II microvesicles mobilized by P2X7R activation

The biological functions of exosomes characterized thus far in various cell types include antigen presentation, exchange of genetic materials such as mRNA and microRNA, proinflammatory stimulation, cell differentiation, utilization as biomarkers for different diseases, and transport of alloantigens between donor and recipient DCs during organ transplantation (20–23,54–57). The rapid secretion of MHC-II microvesicles and exosomes from P2X7R-activated macrophages may provide an efficient route not only for releasing proinflammatory cytokines, but also for rapid dissemination and presentation of foreign antigens as part of an adaptive immune response that is coordinated with local inflammation. In this regard, it is interesting to note very recent studies reporting that alum, the classical adjuvant used in vaccine development, activates the same ASC/NLRP3 inflammasome targeted by P2X7R (50,58). The ability of activated P2X7R to trigger rapid release of a significant mass of MHC-II containing membranes suggests a link between the well-established role of this receptor in innate immune responses and a possible role in potentiating adaptive immune responses.

Supplementary Material

Refer to Web version on PubMed Central for supplementary material.

Acknowledgments

The authors thank Dr. Hisashi Fujioka for preparation, execution, and interpretation of electron microscopy experiments.

References

1. Di Virgilio F. Liaisons dangereuses: P2X(7) and the inflammasome. Trends Pharmacol Sci 2007;28:465–472. [PubMed: 17692395]
2. Mariathasan S, Newton K, Monack DM, Vucic D, French DM, Lee WP, Roose-Girma M, Erickson S, Dixit VM. Differential activation of the inflammasome by caspase-1 adaptors ASC and Ipaf. Nature 2004;430:213–218. [PubMed: 15190255]
3. Mariathasan S, Weiss DS, Newton K, McBride J, O'Rourke K, Roose-Girma M, Lee WP, Weinrauch Y, Monack DM, Dixit VM. Cryopyrin activates the inflammasome in response to toxins and ATP. Nature. 2006
4. Qu Y, Franchi L, Nunez G, Dubyak GR. Nonclassical IL-1 beta secretion stimulated by P2X7 receptors is dependent on inflammasome activation and correlated with exosome release in murine macrophages. J Immunol 2007;179:1913–1925. [PubMed: 17641058]
5. Verhoef PA, Estacion M, Schilling W, Dubyak GR. P2X7 receptor-dependent blebbing and the activation of Rho-effector kinases, caspases, and IL-1 beta release. J Immunol 2003;170:5728–5738. [PubMed: 12759456]
6. Baroni M, Pizzirani C, Pinotti M, Ferrari D, Adinolfi E, Calzavarini S, Caruso P, Bernardi F, Di Virgilio F. Stimulation of P2 (P2X7) receptors in human dendritic cells induces the release of tissue factor-bearing microparticles. Faseb J 2007;21:1926–1933. [PubMed: 17314141]
7. MacKenzie A, Wilson HL, Kiss-Toth E, Dower SK, North RA, Surprenant A. Rapid secretion of interleukin-1beta by microvesicle shedding. Immunity 2001;15:825–835. [PubMed: 11728343]
8. Bianco F, Pravettoni E, Colombo A, Schenk U, Moller T, Matteoli M, Verderio C. Astrocyte-Derived ATP Induces Vesicle Shedding and IL-1{beta} Release from Microglia. J Immunol 2005;174:7268–7277. [PubMed: 15905573]

9. Mutini C, Falzoni S, Ferrari D, Chiozzi P, Morelli A, Baricordi OR, Collo G, Ricciardi-Castagnoli P, Di Virgilio F. Mouse dendritic cells express the P2X7 purinergic receptor: characterization and possible participation in antigen presentation. J Immunol 1999;163:1958–1965. [PubMed: 10438932]
10. Swanberg M, Lidman O, Padyukov L, Eriksson P, Akesson E, Jagodic M, Lobell A, Khademi M, Borjesson O, Lindgren CM, Lundman P, Brookes AJ, Kere J, Luthman H, Alfredsson L, Hillert J, Klareskog L, Hamsten A, Piehl F, Olsson T. MHC2TA is associated with differential MHC molecule expression and susceptibility to rheumatoid arthritis, multiple sclerosis and myocardial infarction. Nat Genet 2005;37:486–494. [PubMed: 15821736]
11. Viville S, Neefjes J, Lotteau V, Dierich A, Lemeur M, Ploegh H, Benoist C, Mathis D. Mice lacking the MHC class II-associated invariant chain. Cell 1993;72:635–648. [PubMed: 7679955]
12. Neefjes JJ, Stollorz V, Peters PJ, Geuze HJ, Ploegh HL. The biosynthetic pathway of MHC class II but not class I molecules intersects the endocytic route. Cell 1990;61:171–183. [PubMed: 2156628]
13. Geuze HJ. The role of endosomes and lysosomes in MHC class II functioning. Immunol Today 1998;19:282–287. [PubMed: 9639994]
14. Kleijmeer M, Ramm G, Schuurhuis D, Griffith J, Rescigno M, Ricciardi-Castagnoli P, Rudensky AY, Ossendorp F, Melief CJ, Stoorvogel W, Geuze HJ. Reorganization of multivesicular bodies regulates MHC class II antigen presentation by dendritic cells. J Cell Biol 2001;155:53–63. [PubMed: 11581285]
15. Morelli AE, Larregina AT, Shufesky WJ, Sullivan ML, Stolz DB, Papworth GD, Zahorchak AF, Logar AJ, Wang Z, Watkins SC, Falo LD Jr, Thomson AW. Endocytosis, intracellular sorting, and processing of exosomes by dendritic cells. Blood 2004;104:3257–3266. [PubMed: 15284116]
16. Raposo G, Nijman HW, Stoorvogel W, Liejendekker R, Harding CV, Melief CJ, Geuze HJ. B lymphocytes secrete antigen-presenting vesicles. J Exp Med 1996;183:1161–1172. [PubMed: 8642258]
17. Thery C, Duban L, Segura E, Veron P, Lantz O, Amigorena S. Indirect activation of naive CD4+ T cells by dendritic cell-derived exosomes. Nat Immunol 2002;3:1156–1162. [PubMed: 12426563]
18. Quah BJ, O'Neill HC. The immunogenicity of dendritic cell-derived exosomes. Blood Cells Mol Dis 2005;35:94–110. [PubMed: 15975838]
19. Li XB, Zhang ZR, Schluesener HJ, Xu SQ. Role of exosomes in immune regulation. J Cell Mol Med 2006;10:364–375. [PubMed: 16796805]
20. Valadi H, Ekstrom K, Bossios A, Sjostrand M, Lee JJ, Lotvall JO. Exosome-mediated transfer of mRNAs and microRNAs is a novel mechanism of genetic exchange between cells. Nat Cell Biol 2007;9:654–659. [PubMed: 17486113]
21. Sanderson MP, Keller S, Alonso A, Riedle S, Dempsey PJ, Altevogt P. Generation of novel, secreted epidermal growth factor receptor (EGFR/ErbB1) isoforms via metalloprotease-dependent ectodomain shedding and exosome secretion. J Cell Biochem 2008;103:1783–1797. [PubMed: 17910038]
22. Izquierdo-Useros N, Naranjo-Gomez M, Archer J, Hatch SC, Erkizia I, Blanco J, Borras FE, Puertas MC, Connor JH, Fernandez-Figueras MT, Moore L, Clotet B, Gummuluru S, Martinez-Picado J. Capture and transfer of HIV-1 particles by mature dendritic cells converges with the exosome-dissemination pathway. Blood. 2008
23. Bhatnagar S, Shinagawa K, Castellino FJ, Schorey JS. Exosomes released from macrophages infected with intracellular pathogens stimulate a proinflammatory response in vitro and in vivo. Blood 2007;110:3234–3244. [PubMed: 17666571]
24. Shin JS, Ebersold M, Pypaert M, Delamarre L, Hartley A, Mellman I. Surface expression of MHC class II in dendritic cells is controlled by regulated ubiquitination. Nature 2006;444:115–118. [PubMed: 17051151]
25. van Niel G, Wubbolts R, Ten Broeke T, Buschow SI, Ossendorp FA, Melief CJ, Raposo G, van Balkom BW, Stoorvogel W. Dendritic cells regulate exposure of MHC class II at their plasma membrane by oligoubiquitination. Immunity 2006;25:885–894. [PubMed: 17174123]
26. Segura E, Nicco C, Lombard B, Veron P, Raposo G, Batteux F, Amigorena S, Thery C. ICAM-1 on exosomes from mature dendritic cells is critical for efficient naive T-cell priming. Blood 2005;106:216–223. [PubMed: 15790784]

27. Saunderson SC, Schuberth PC, Dunn AC, Miller L, Hock BD, MacKay PA, Koch N, Jack RW, McLellan AD. Induction of exosome release in primary B cells stimulated via CD40 and the IL-4 receptor. J Immunol 2008;180:8146–8152. [PubMed: 18523279]
28. Fang Y, Wu N, Gan X, Yan W, Morrell JC, Gould SJ. Higher-order oligomerization targets plasma membrane proteins and HIV gag to exosomes. PLoS Biol 2007;5:e158. [PubMed: 17550307]
29. Dowds TA, Masumoto J, Zhu L, Inohara N, Nunez G. Cryopyrin-induced interleukin 1beta secretion in monocytic cells: enhanced activity of disease-associated mutants and requirement for ASC. J Biol Chem 2004;279:21924–21928. [PubMed: 15020601]
30. Myers AJ, Eilertson B, Fulton SA, Flynn JL, Canaday DH. The purinergic P2X7 receptor is not required for control of pulmonary Mycobacterium tuberculosis infection. Infect Immun 2005;73:3192–3195. [PubMed: 15845532]
31. Davies JQ, Gordon S. Isolation and culture of murine macrophages. Methods Mol Biol 2005;290:91–103. [PubMed: 15361657]
32. Kahlenberg JM, Lundberg KC, Kertesy SB, Qu Y, Dubyak GR. Potentiation of caspase-1 activation by the P2X7 receptor is dependent on TLR signals and requires NF-kappaB-driven protein synthesis. J Immunol 2005;175:7611–7622. [PubMed: 16301671]
33. Verhoef PA, Kertesy SB, Lundberg K, Kahlenberg JM, Dubyak GR. Inhibitory effects of chloride on the activation of caspase-1, IL-1beta secretion, and cytolysis by the P2X7 receptor. J Immunol 2005;175:7623–7634. [PubMed: 16301672]
34. del Rey A, Renigunta V, Dalpke AH, Leipziger J, Matos JE, Robaye B, Zuzarte M, Kavelaars A, Hanley PJ. Knock-out mice reveal the contributions of P2Y and P2X receptors to nucleotide-induced Ca2+ signaling in macrophages. J Biol Chem 2006;281:35147–35155. [PubMed: 16980298]
35. Solle M, Labasi J, Perregaux DG, Stam E, Petrushova N, Koller BH, Griffiths RJ, Gabel CA. Altered cytokine production in mice lacking P2X(7) receptors. J Biol Chem 2001;276:125–132. [PubMed: 11016935]
36. Labasi JM, Petrushova N, Donovan C, McCurdy S, Lira P, Payette MM, Brissette W, Wicks JR, Audoly L, Gabel CA. Absence of the P2X7 receptor alters leukocyte function and attenuates an inflammatory response. J Immunol 2002;168:6436–6445. [PubMed: 12055263]
37. Le Feuvre RA, Brough D, Iwakura Y, Takeda K, Rothwell NJ. Priming of macrophages with lipopolysaccharide potentiates P2X7-mediated cell death via a caspase-1-dependent mechanism, independently of cytokine production. J Biol Chem 2002;277:3210–3218. [PubMed: 11706016]
38. Schotte P, Declercq W, Van Huffel S, Vandenabeele P, Beyaert R. Non-specific effects of methyl ketone peptide inhibitors of caspases. FEBS Lett 1999;442:117–121. [PubMed: 9923616]
39. Pereira NA, Song Z. Some commonly used caspase substrates and inhibitors lack the specificity required to monitor individual caspase activity. Biochem Biophys Res Commun 2008;377:873–877. [PubMed: 18976637]
40. Thery C, Regnault A, Garin J, Wolfers J, Zitvogel L, Ricciardi-Castagnoli P, Raposo G, Amigorena S. Molecular characterization of dendritic cell-derived exosomes. Selective accumulation of the heat shock protein hsc73. J Cell Biol 1999;147:599–610. [PubMed: 10545503]
41. Muntasell A, Berger AC, Roche PA. T cell-induced secretion of MHC class II-peptide complexes on B cell exosomes. Embo J 2007;26:4263–4272. [PubMed: 17805347]
42. Pizzirani C, Ferrari D, Chiozzi P, Adinolfi E, Sandona D, Savaglio E, Di Virgilio F. Stimulation of P2 receptors causes release of IL-1beta-loaded microvesicles from human dendritic cells. Blood 2007;109:3856–3864. [PubMed: 17192399]
43. Segura E, Amigorena S, Thery C. Mature dendritic cells secrete exosomes with strong ability to induce antigen-specific effector immune responses. Blood Cells Mol Dis 2005;35:89–93. [PubMed: 15990342]
44. Hristov M, Erl W, Linder S, Weber PC. Apoptotic bodies from endothelial cells enhance the number and initiate the differentiation of human endothelial progenitor cells in vitro. Blood 2004;104:2761–2766. [PubMed: 15242875]
45. Escola JM, Kleijmeer MJ, Stoorvogel W, Griffith JM, Yoshie O, Geuze HJ. Selective enrichment of tetraspan proteins on the internal vesicles of multivesicular endosomes and on exosomes secreted by human B-lymphocytes. J Biol Chem 1998;273:20121–20127. [PubMed: 9685355]

46. Bunbury A, Potolicchio I, Maitra R, Santambrogio L. Functional analysis of monocyte MHC class II compartments. Faseb J. 2008
47. Fernandes-Alnemri T, Wu J, Yu JW, Datta P, Miller B, Jankowski W, Rosenberg S, Zhang J, Alnemri ES. The pyroptosome: a supramolecular assembly of ASC dimers mediating inflammatory cell death via caspase-1 activation. Cell Death Differ 2007;14:1590–1604. [PubMed: 17599095]
48. Willingham SB, Bergstralh DT, O'Connor W, Morrison AC, Taxman DJ, Duncan JA, Barnoy S, Venkatesan MM, Flavell RA, Deshmukh M, Hoffman HM, Ting JP. Microbial pathogen-induced necrotic cell death mediated by the inflammasome components CIAS1/cryopyrin/NLRP3 and ASC. Cell Host Microbe 2007;2:147–159. [PubMed: 18005730]
49. Suzuki T, Franchi L, Toma C, Ashida H, Ogawa M, Yoshikawa Y, Mimuro H, Inohara N, Sasakawa C, Nunez G. Differential regulation of caspase-1 activation, pyroptosis, and autophagy via Ipaf and ASC in Shigella-infected macrophages. PLoS Pathog 2007;3:e111. [PubMed: 17696608]
50. Hornung V, Bauernfeind F, Halle A, Samstad EO, Kono H, Rock KL, Fitzgerald KA, Latz E. Silica crystals and aluminum salts activate the NALP3 inflammasome through phagosomal destabilization. Nat Immunol 2008;9:847–856. [PubMed: 18604214]
51. Halle A, Hornung V, Petzold GC, Stewart CR, Monks BG, Reinheckel T, Fitzgerald KA, Latz E, Moore KJ, Golenbock DT. The NALP3 inflammasome is involved in the innate immune response to amyloid-beta. Nat Immunol 2008;9:857–865. [PubMed: 18604209]
52. Subra C, Laulagnier K, Perret B, Record M. Exosome lipidomics unravels lipid sorting at the level of multivesicular bodies. Biochimie 2007;89:205–212. [PubMed: 17157973]
53. Trajkovic K, Hsu C, Chiantia S, Rajendran L, Wenzel D, Wieland F, Schwille P, Brugger B, Simons M. Ceramide triggers budding of exosome vesicles into multivesicular endosomes. Science 2008;319:1244–1247. [PubMed: 18309083]
54. Yu S, Liu C, Su K, Wang J, Liu Y, Zhang L, Li C, Cong Y, Kimberly R, Grizzle WE, Falkson C, Zhang HG. Tumor exosomes inhibit differentiation of bone marrow dendritic cells. J Immunol 2007;178:6867–6875. [PubMed: 17513735]
55. Vella LJ, Sharples RA, Nisbet RM, Cappai R, Hill AF. The role of exosomes in the processing of proteins associated with neurodegenerative diseases. Eur Biophys J 2008;37:323–332. [PubMed: 18064447]
56. Pisitkun T, Shen RF, Knepper MA. Identification and proteomic profiling of exosomes in human urine. Proc Natl Acad Sci U S A 2004;101:13368–13373. [PubMed: 15326289]
57. Montecalvo A, Shufesky WJ, Stolz DB, Sullivan MG, Wang Z, Divito SJ, Papworth GD, Watkins SC, Robbins PD, Larregina AT, Morelli AE. Exosomes as a short-range mechanism to spread alloantigen between dendritic cells during T cell allorecognition. J Immunol 2008;180:3081–3090. [PubMed: 18292531]
58. Li H, Willingham SB, Ting JP, Re F. Cutting edge: inflammasome activation by alum and alum's adjuvant effect are mediated by NLRP3. J Immunol 2008;181:17–21. [PubMed: 18566365]
59. Auger R, Motta I, Benihoud K, Ojcius DM, Kanellopoulos JM. A role for mitogen-activated protein kinase(Erk1/2) activation and non-selective pore formation in P2X7 receptor-mediated thymocyte death. J Biol Chem 2005;280:28142–28151. [PubMed: 15937334]

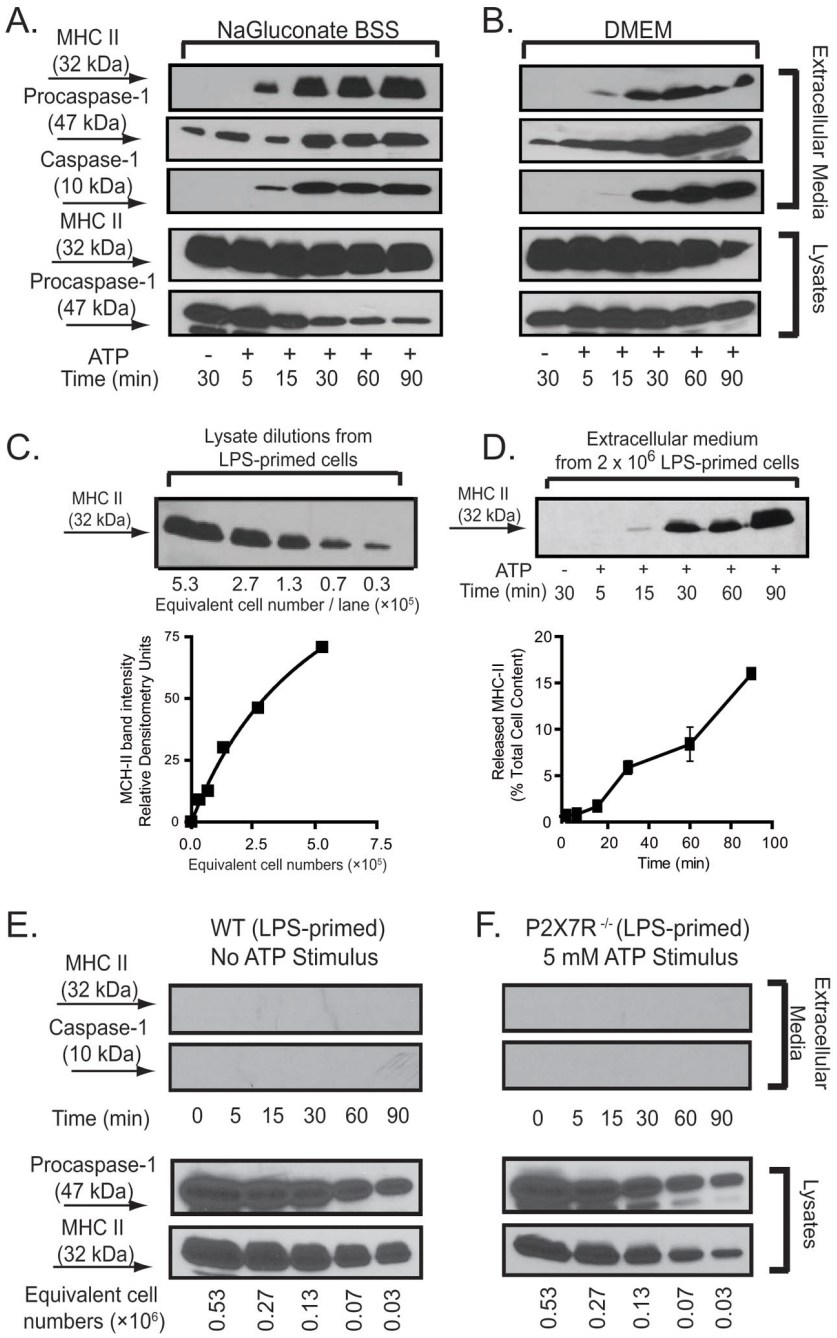

Figure 1. P2X7R-dependent release of MHC-II from inflammatory murine BMDM

A, B. C57BL/6 BMDM were plated 2× 10^6/well, and pretreated with IFN-γ (2 ng/ml) for 16–18 h before LPS (1 μg/ml) priming for 4 h. Cells were transferred to either BSS or DMEM and stimulated with 5 mM ATP for the indicated times. The extracellular media and cell lysates were separately collected and processed for western blot analysis. The blot membrane was first probed with anti-MHC-II antibody, then stripped and sequentially probed with antibodies against caspase-1. These data are representative of similar time course studies from 6 separate experiments with BSS and 4 separate experiments with DMEM. C. A standard curve was generated from a series of dilutions corresponding to the indicated number of IFN–γ and LPS-primed BMDM per lane. Densitometric analysis performed with Image J version 1.39u imaging

software (59) was used to correlate MHC-II band intensities with corresponding cell number. D. IFN–γ and LPS-primed BMDM were stimulated without or with 5 mM ATP for the indicated times and the released MHC-II was quantified as the percentage of total cellular MHC-II content based on the panel C standard curve The data points in the bottom panel represent the means±SE from 8 experiments using different preparations of C57BL/6 BMDM; the western blot in the upper panel is from a representative experiment. E. IFN–γ and LPS-primed BMDM from wildtype C57BL/6 mice were transferred to BSS and incubated for the indicated times in the absence of ATP stimulation. The extracellular media samples collected at each time point were processed for analysis of MHC-II and caspase-1 content. Serial dilutions of the cell lysates were processed in parallel for analysis of total cellular MHC-II content. The western blot data are representative of observations from 3 separate experiments. F. IFN–γ and LPS-primed BMDM from P2X7R-knockout ($P2X7R^{-/-}$) mice were transferred to BSS and stimulated for the indicated times in the presence of 5 mM. The extracellular media samples collected at each time point were processed for analysis of MHC-II and caspase-1 content. Serial dilutions of the cell lysates were processed in parallel for analysis of total cellular MHC-II content. These data are representative of observations from 5 separate experiments.

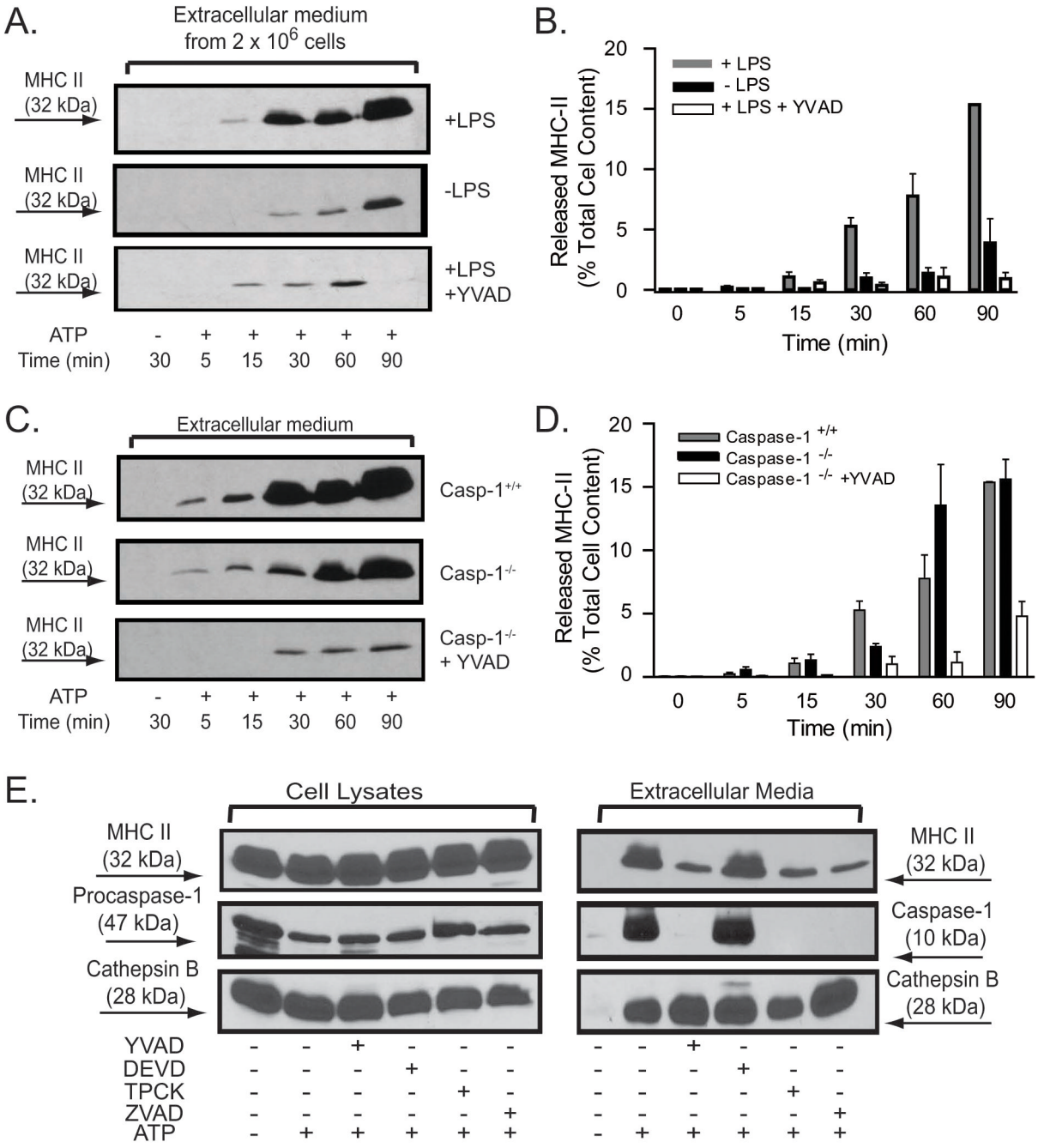

Figure 2. P2X7R-induced release of MHC-II is potentiated by LPS priming and suppressed by peptide inhibitors of proteases but is independent of caspase-1

A, B. BMDM from wildtype C57BL/6 mice were pretreated with IFN-γ (2 ng/ml) for 16–18 h before priming with or without LPS (1 μg/ml) for 4 hr. The primed BMDM were then stimulated without or with 5 mM ATP for the indicated times in the absence or presence of 50 YVAD-cmk. The released MHC-II at each time point was quantified as the percentage of total cellular MHC-II content using the protocol in Figs. 1C and D. The data points in panel B represent the means±SE from 8 experiments that tested the effects of priming and 6 experiments that tested the effects of the YVAD-cmk inhibitor; the western blots in panel A are from representative experiments. C, D. BMDM from wildtype C57BL/6 mice (WT) or

caspase$^{-/-}$mice were pretreated with IFN-γ (2 ng/ml) for 16–18 h before priming with LPS (1 μg/ml) for 4 hr. The primed BMDM were then stimulated without or with 5 mM ATP for the indicated times in the absence or presence of 50 μM YVAD-cmk. The released MHC-II at each time point was quantified as the percentage of total cellular MHC-II content using the protocol in Fig. 1C and D The data points in panel D represent the means±SE from 8 experiments with WT BMDM, 5 experiments with caspase-1$^{-/-}$ BMDM, and 4 experiments with caspase-1$^{-/-}$ BMDM treated with YVAD-cmk; the western blots in panel C are from representative experiments. E.. IFN–γ and LPS-primed BMDM from wildtype C57BL/6 mice were transferred to BSS and incubated with or without 50 μM YVAD-cmk, 50 μM DEVD-cho, 50 μM ZVAD-fmk, or 100 μM TPCK for 30 min prior to stimulation with 5 mM ATP for an additional 30 min. The extracellular media and cell lysates were separately collected and processed for western blot analysis of MHC-II, caspase-1, and cathepsin B. The data are representative of results from 3 separate experiments.

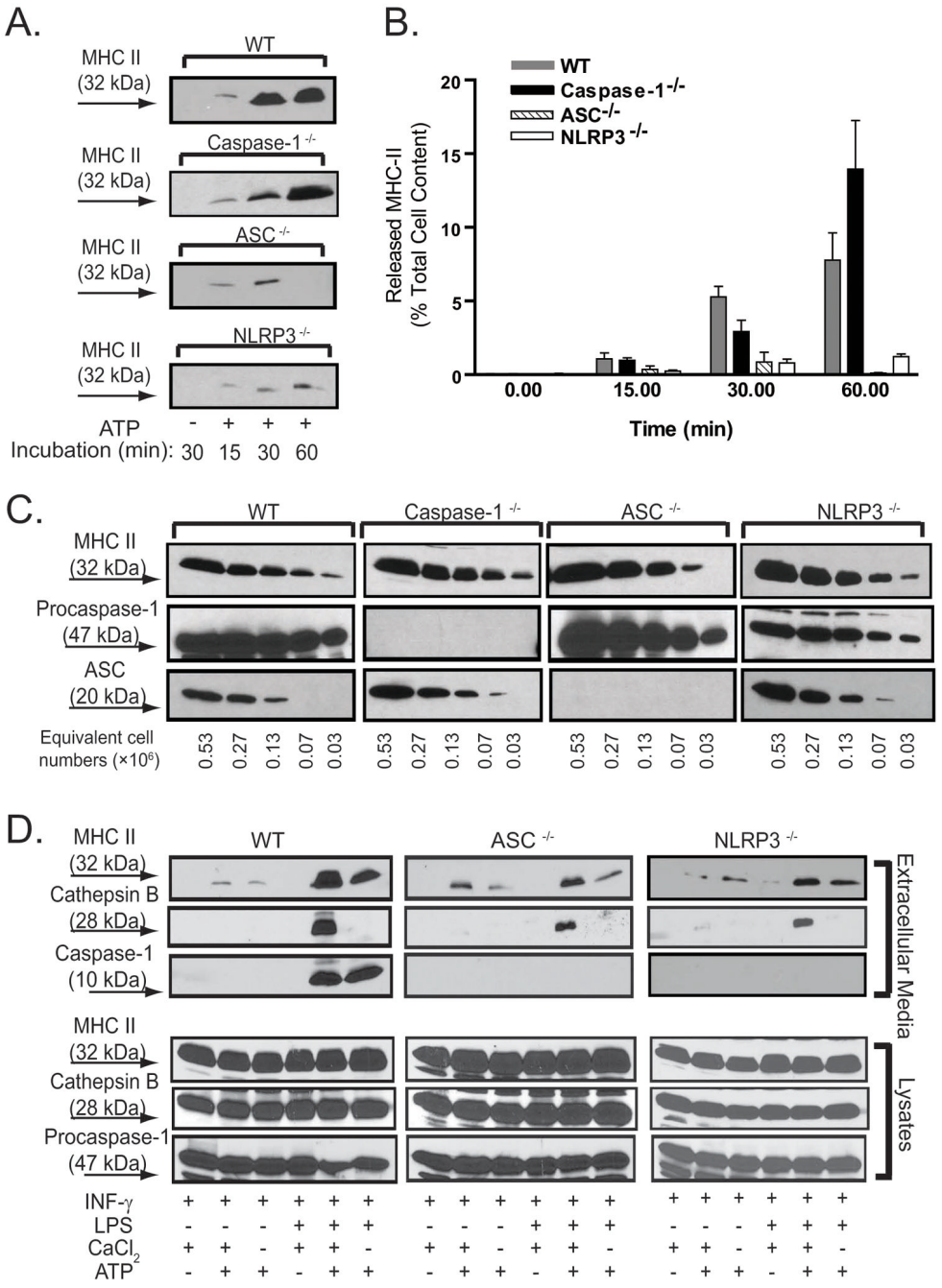

Figure 3. The inflammasome proteins, ASC and NLRP3, but not caspase-1, are required for maximal P2X7R-induced release of MHC-II

A., B. BMDM from WT, caspase-1$^{-/-}$, ASC$^{-/-}$, and NLRP3$^{-/-}$ mice were pretreated with IFN-γ (2 ng/ml) for 16–18 h prior to LPS (1 μg/ml) priming for 4 h. The primed BMDM were then stimulated without or with 5 mM ATP for the indicated times in the absence or presence of 50 μM YVAD-cmk. The released MHC-II at each time point was quantified as the percentage of total cellular MHC-II content using the protocol in Figs. 1C and D. The data points in panel B represent the means±SE from 8 experiments with WT BMDM, 7 experiments each with ASC$^{-/-}$and NLRP3$^{-/-}$ BMDM, and 5 experiments with caspase-1$^{-/-}$ BMDM; the western blots in panel A are from representative experiments. The cells were transferred to BSS, and

stimulated with 5 mM ATP for indicated times. The extracellular media and cell lysates were collected and processed for semi-quantitative western blot analysis. C. Lysate dilutions from WT, caspase-$1^{-/-}$, $ASC^{-/-}$, $NLRP3^{-/-}$ BMDM were analyzed for their relative contents of MHC-II, procaspase-1 and ASC. D. BMDM from WT, $ASC^{-/-}$, and $NLRP3^{-/-}$ mice were pretreated with IFN-γ (2 ng/ml) for 16–18 h prior to additional incubation without or with LPS (1 μg/ml) for 4 h. The cells were transferred to either Ca^{2+}-containing or Ca^{2+}-free BSS, and then stimulated with or without 5 mM ATP for 5 min. The extracellular media and cell lysates were collected and processed for western blot analysis of MHC-II, caspase-1, and cathepsin B. The data are representative of observations from 5 experiments.

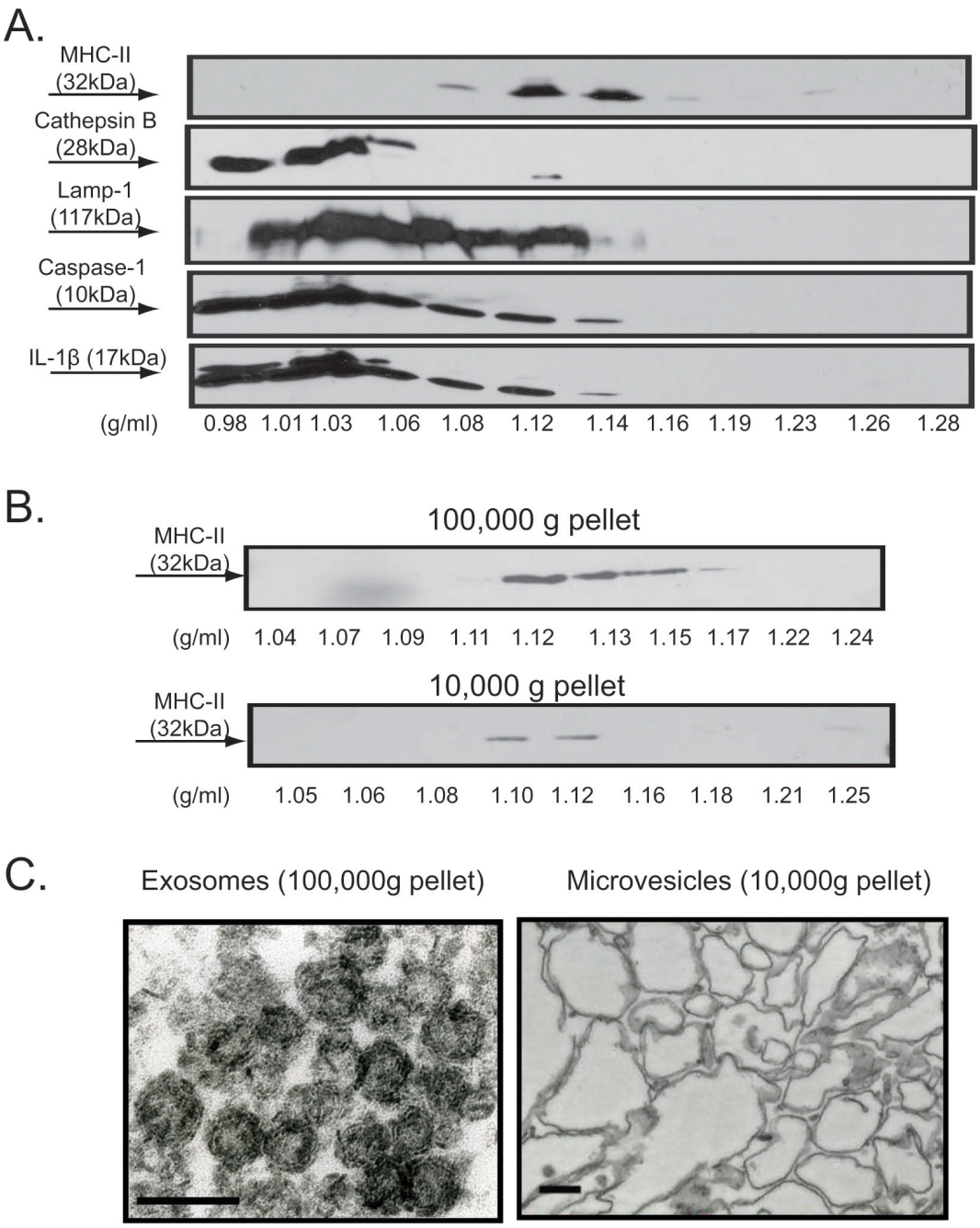

Figure 4. P2X7R-induced release of MHC-II containing membranes includes both microvesicles and exosomes

A. 30 ~ 40 × 10^6 BMDM were pretreated with IFN-γ (2 ng/ml) for 16–18 h prior to LPS (1 μg/ml) priming for 4 h. The cells were transferred to BSS, and then stimulated with 5 mM ATP for 15 min. The collected extracellular media were centrifuged successively at 300×g and 2000×g, concentrated by using CENTRIPREP, followed by layering on top of linear sucrose density gradients and overnight centrifugation. Each fraction from the sucrose gradient was weighed and then subjected to western blot analysis. The membrane was sequentially probed with anti-MHC-II, anti-caspase-1, anti-IL-1β, anti-LAMP-1, and anti-cathepsin B. Data are representative of results from 2 experiments. B. IFN-γ and LPS-primed BMDM were

transferred to BSS and stimulated with 5 mM ATP for 15 min. The extracellular media was collected, sequentially centrifuged at 300×g, 2000×g, 10,000×g, and 100,000×g. The pellets from the 10,000×g, and 100,000×g spins processed by equilibrium sucrose density gradient centrifugation and the resulting fractions analyzed by western blot. The results are representative of 2 experiments. C. IFN–γ and LPS-primed BMDM were stimulated with 5 mM ATP for 15 min. The extracellular media was collected, sequentially centrifuged at 300×g, 2000×g, 10,000×g, and 100,000×g. The microvesicles obtained from the 10,000×g pellet and the exosomes obtained from the 100,000×g pellet were analyzed by electron microscopy. The scale bars are 100 nm and the the images are representative of observations from 2 experiments.

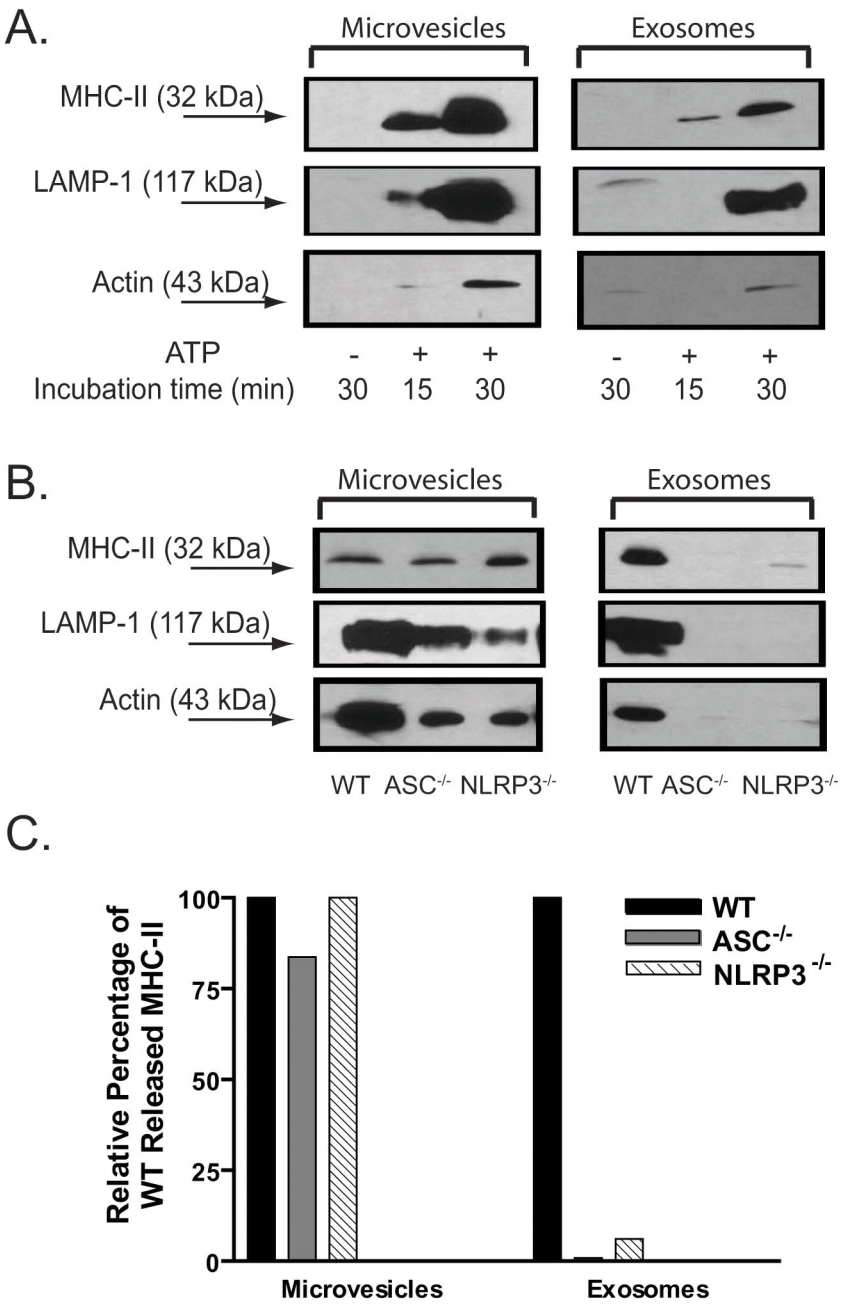

Figure 5. The ASC and NLRP3 inflammasome proteins are required for P2X7R-induced release of MHC-II exosomes but not MHC-II microvesicles

A. IFN-γ and LPS-primed BMDM were stimulated without ATP for 30 min or with ATP for 30 min. The extracellular media was collected, sequentially centrifuged at 300×g, 2000×g, 10,000×g, and 100,000×g. The microvesicles obtained from the 10,000×g pellet and the exosomes obtained from the 100,000×g pellet were analyzed by western blot analysis. The membrane was probed sequentially with antibodies against MHC-II, caspase-1, LAMP-1, and actin. The results are representative of observations from 3 experiments. B. IFN–γ and LPS-primed BMDM WT, ASC$^{-/-}$, or NLRP3$^{-/-}$ mice were stimulated with 5 mM ATP for 30 min. The extracellular media fractions were collected and sequentially centrifuged at 300×g, 2000×g,, and 100,000×g. The microvesicles obtained from the 10,000×g pellet and the

exosomes obtained from the 100,000×g pellet were analyzed by western blot analysis. The membrane was probed sequentially with antibodies against MHC-II, LAMP-1, and actin. The results are representative of data from 3 experiments with WT and 2 experiments each with $ASC^{-/-}$ or $NLRP3^{-/-}$ BMDM. C. The MHC-II bands from the western blot data in panel B were quantified by densitometry. The MHC-II band densities from the $ASC^{-/-}$ and $NLRP3^{-/-}$ sample lanes were normalized to the band densities measured in the WT sample lanes.

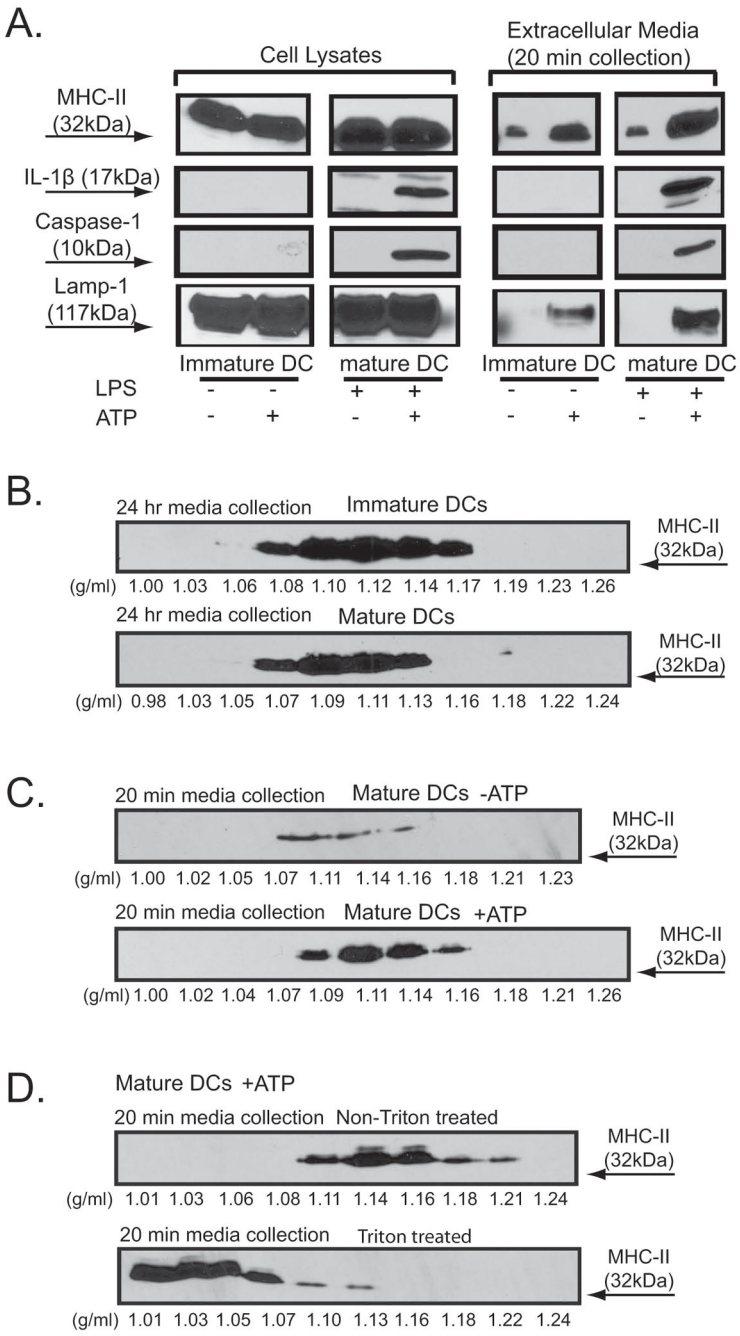

Figure 6. Comparison of MHC-II membranes released from immature and mature BMDC via constitutive or ATP-stimulated mechanisms

A. BMDC derived from C57BL/6 mice were primed with LPS (1 μg/ml) for 4 h, transferred to BSS, and stimulated with or without 5 mM ATP for 15 min. The extracellular media and the cell lysates were processed and analyzed by western blot sequentially probed with antibodies against MHC-II, caspase-1, IL-1β, and LAMP-1. The results are representative of observations from 3 experiments. B. C. D. BMDC were primed either without (for immature DC) or with 1 μg/ml LPS (for mature DC) for 24 h before further experimentation. B. Immature or mature DC was incubated in serum-free DMEM media for 24 hr before collection and processing of the extracellular fraction. C. D. Mature DC were transferred to BSS and

stimulated either with or without 5 mM ATP for 20 min before collection and processing of the extracellular fraction. The collected extracellular media were sequentially centrifuged to eliminate dead cells and debris, followed by concentration. In panels B and C, the concentrated samples were directly loaded onto linear sucrose gradients. D. The concentrated medium samples were supplemented with or without Triton X-100 before loading onto linear sucrose gradients. The sucrose gradient samples were then centrifuged at 100,000×g for 16 h. 1 ml fractions were collected, weighed, precipitated by TCA, and analyzed by western blot.